DIRECT MEASUREMENT OF THE INITIAL PROTON EXTRUSION TO OXYGEN UPTAKE RATIO ACCOMPANYING SUCCINATE OXIDATION BY RAT LIVER MITOCHONDRIA

ORUGANTI H. SETTY,* RICHARD I. SHRAGER,‡ BARRY BUNOW,‡ BALTAZAR REYNAFARJE,§ ALBERT L. LEHNINGER,§† AND RICHARD W. HENDLER*

Laboratory of Cell Biology, National Heart, Lung, and Blood Institute, National Institutes of Health, Building 3, Room B1-22, Bethesda, Maryland 20205; ‡Laboratory of Applied Studies, Division of Computer Research and Technology, National Institutes of Health; and §Department of Physiological Chemistry, The Johns Hopkins University School of Medicine, Baltimore, Maryland 21205

ABSTRACT The problem of obtaining very early ratios for the H^+/O stoichiometry accompanying succinate oxidation by rat liver mitochondria was attacked using new techniques for direct measurement rather than extrapolations based on data obtained after mixing and the recovery of the electrode from the initial injection of O_2. Respiration was quickly initiated in a thoroughly mixed O_2-containing suspension of mitochondria under a CO atmosphere by photolysis of the CO-cytochrome *c* oxidase complex-. Fast responding O_2 and pH electrodes were used to collect data every 10 ms. The response time for each electrode was experimentally measured in each experiment and suitable corrections for electrode relaxations were made. With uncorrected data obtained after 0.8 s, the extrapolation back to zero time on the basis of single-exponential curve fitting confirmed values close to 8.0 as previously reported (Costa et al., 1984). The data directly obtained, however, indicate an initial burst in H^+/O ratio that peaked to values of ~20 to 30 prior to 50 ms and which was no longer evident after 0.3 s. Newer information and considerations that place all extrapolation methods in question are discussed.

INTRODUCTION

The determination of H^+/O stoichiometries characteristic of the oxidation of particular substrates is subject to difficult experimental problems that have not been satisfactorily resolved. It is known that after the first protons have been translocated, the developing $\Delta\tilde{\mu}_{H^+}$ retards further translocation and enhances the leak of previously translocated protons back to the vesicle interior. Therefore, the best estimate of H^+/O stoichiometry is obtained as close to the start of a respiratory pulse as possible. Methods that relate the bulk discharge of protons to the total amount of O_2 consumed must necessarily produce ratios that are too low. Attempts to correct such estimates for a calculated amount of backflow involve assumptions of questionable validity. A more dependable approach is to measure actual simultaneous rates of proton translocation and O_2 uptake. In this approach, however, part of the record during the first second has been unattainable because of the time of mixing of the O_2-containing aliquot, which is usually added to initiate the burst of respiration, and because of the time required by the O_2 electrode to recover after responding to the initial injection. With the assumptions that the changes in H^+ and O_2 concentrations in the medium from ~0.8 to 5 s are monotonic and characteristic of the changes occurring from zero time, initial H^+/O ratios can be estimated. A previously undiscussed weakness in this approach is that zero time is not a sharply defined instant. At the end of the mixing period there is a myriad of exposure times of individual mitochondria to O_2. We have eliminated the mixing time by starting the respiratory pulse with photolysis of the CO-cytochrome oxidase complex in an already mixed suspension of mitochondria and O_2. Data were collected from zero time at 10-ms intervals from fast responding O_2 and pH electrodes. The ability to collect such early data from electrodes requires corrections for the response time delays of the electrodes to relate the signals to actual concentrations of H^+ and O_2. These corrections have been made based on the experimentally determined relaxation constants of each electrode. A preliminary report of this work has been published (1).

EXPERIMENTAL PROCEDURES

General Description of the System

The glass reaction vessel consisted of an inner chamber surrounded by a water jacket (2). The mitochondrial suspension (total volume, 6.0 ml) was

Correspondence should be addressed to Richard W. Hendler.

†Deceased March 4, 1986.

stirred with a Teflon-coated magnetic bar under a gas phase of 100% carbon monoxide. A glass pH electrode and a Davies-type rapid response O_2 electrode (3) with an auxiliary elec trode (WP Instruments, Inc., MERE-1 Reference Electrode, New Haven, CT) were held in place by snug Teflon sleeves. In the experiments in series N1, an Ingold combination electrode (LOT-405-M5) was used, and for the other experimental groups, an Ingold glass electrode (LOT-275-M5) was used. The vessel was housed in a light-tight, metal Faraday cage which was electrically grounded to the chassis of the electronic interface which received the electrode signals. A quartz halogen filament lamp (model 6333; Oriel Corp., Stamford, CT) in a housing adapted from an Aminco Chance spectrophotometer was focused through a lens system in a 4-cm diameter metal tube which provided for uniform illumination over the face of the reaction vessel. A camera shutter operated with a cable release was opened to illuminate the sample. In this way, electron flow from succinate to dissolved O_2 ($\leq$ 10 μM), already in the medium containing the mitochondria, could be initiated at the desired instant by photolysis of the carbon monoxide-cytochrome oxidase complex. The Faraday cage was an important part of the many noise reduction measures taken to allow the accurate measurement of changes of 50-100 μV in electrode signals which occurred during the first 100 ms of respiration. The electrodes were connected to a specially designed interface (2) which performed several functions. The interface decreased noise by a common mode rejection between the reference and pH electrodes and by a stage of electronic low pass filtering. The interface contained a circuit for driving a shield surrounding the pH cable with a voltage equal to that of the pH signal, thus decreasing capacitance and speeding electrode response. Finally both offset and amplification were provided to modify the signals for subsequent input to an A/D converter.

A major source of noise was traced to the pH electrode itself, which was initially a combination type. The stirred solution moving across the liquid junction of the reference electrode caused changes in junction potential, thus producing significant fluctuations in background voltage. This source of noise was eliminated by replacing the combination electrode with a pH glass electrode and placing its reference electrode, described above, in a separate unstirred tube containing the working buffer. Electrical connection between the reference compartment and the mitochondrial suspension was provided by a bridge of 4% agar in the working buffer, cast in "Intramedic No. 7440" polyethylene tubing. The pH cable was shielded with a grounded outer shield external to the electrically driven inner shield. The glass pH electrode contained an outer compartment filled with a salt solution that was electrically connected to the outer shield of the electrode. The pH signal emerging from the electronic interface was then filtered electronically to avoid aliasing of high frequencies into the discretized data. For this purpose, a Reactions Instruments, Inc. (Reston, VA) model R7000M variable electronic filter operating as a low-pass Gaussian filter was used. The cutoff frequency (12db down) was 20 Hz with a 24 db-per-octave attenuation rate (i.e., at f = 20 Hz, the response, $H(f)$ = (output voltage)/(input voltage) was 1/4, and thereafter, that ratio proceeded as 1/frequency to the fourth power). A Gaussian filter has a bell shaped $H(f)$ centered at f = 0. Residual 60-cycle noise was greatly reduced by adding KCl to the water which circulated in the jacket around the mitochondrial suspension. The final elimination of noise was accomplished by digital filtering as described below.

The pH signal emerging from the 20 cycle low pass filter and the O_2 electrode signal emerging from the electronic interface were digitized by a 12-bit A/D converter and then passed to a single board Intel 8080 (Intel Corp., Santa Clara, CA) as previously described (2). This system allowed data acquistion from the measuring electrodes at a rate of 100 observations per s per electrode. The accumulated data, which amounted usually to ~3,000 points per experiment, were transferred first to an Intel-MDS development system for storage on disks and then subsequently to a main frame DEC system-10 (PDP-10) for processing.

For the determination of relaxation times of the pH and O_2 electrodes it was necessary to have a means of changing the concentration of H^+ or O_2 within a time-span of ms. The simple addition of acid or oxygenated buffer to a stirred solution could not be used because of the relatively long mixing time. A specifically designed flow cell (to be described separately) was used to accomplish the rapid changes required. A 1 mm diameter channel was bored through a lucite block and tight seals were provided to hold the two electrodes in place with their sensitive tips exposed to the channel. Two separate reference electrodes (as described above), one for each of the measuring electrodes, were placed in a separate chamber in the lucite block. The reference chamber was filled with working buffer and electrically coupled to the main groove by another groove which formed a right angle with the main groove at a point between the measuring electrodes and the exit. The inlet to the block was connected to a Hamilton 3-way valve which was fitted to two syringes. Relaxation times were measured for each batch of mitochondria at the end of each experimental series. The pooled mitochondrial suspension used for this determination was divided into two parts. To one portion (suspension 1) KOH was added to change the pH from 7.05 to 7.5 and the suspension was placed in a syringe to allow it to become anaerobic. Antimycin (2 nmol/ml) was added to the other portion (pH 7.05)(suspension 2), which was allowed to become aerobic. The main channel of the flow cell was filled with suspension 1. After stable pH and O_2 electrode readings, were attained, suspension 1 was quickly displaced by suspension 2 which was contained in the second syringe. The outputs of the electrodes were processed as described above.

Experimental Procedure for H^+/O Ratio Determinations

The buffered medium (4) (~5.5 ml), containing 200 mM sucrose, 50 mM KCl, and 1.5 mM HEPES adjusted to pH 7.05, was placed in the water-jacketed reaction vessel maintained at 25° and made anaerobic by bubbling with a stream of N_2. The N_2 gas was then stopped and 100% carbon monoxide was passed over the surface at a rate of 80 ml/min. Next, rotenone (2.0 μM) and succinate (5.0 mM) were added, followed by rat liver mitochondria (18 mg of protein) in 0.3 ml to adjust the final volume to 6.0 ml. Oxygen admitted during the above additions was removed by illumination of the suspension and allowing O_2 uptake to proceed until the O_2 trace was stable at zero concentration. After 5 min of total anaerobiosis, 18 μg of oligomycin, and 90 μg of N-ethylmaleimide were added, followed in 3 to 5 min by 2.2 μg of valinomycin.

The illumination was stopped by closing the photographic shutter, and the stirred suspension left in the dark for 15 to 20 min under the carbon monoxide atmosphere. A known amount of O_2 in air-saturated buffer (~0.2 ml) was added in the dark. The calibration for the O_2 electrode was taken from this injection. After ~30 s the photographic shutter was opened to initiate electron flow. The subsequent changes in O_2 and H^+ concentrations were then recorded. After the O_2 uptake was complete, the pH electrode was calibrated by injection of 400 nmol HCl. The rat liver mitochondria were prepared in sucrose as in reference 5. The respiratory control index of each preparation was measured by the difference in the rate of succinate oxidation before and after the addition of 0.5 μM FCCP using a standard clark O_2 electrode (model 4004, Yellow Springs Inst. Co., Yellow Springs, OH). These ratios were between 6 and 10 for all preparations of mitochondria used. Protein was determined by the biuret procedure (6).

Data Analysis

An electrode requires a finite time to respond to a change in concentration of the species it measures. If the concentration of the measured ion undergoes continuous change, the electrode reading will always lag behind the true reading by an amount determined by the response characteristic, unique to the electrode, and the rate of the concentration change. The relationship between the true reading of the electrode, Z, and the observed reading, Y, can be represented as

$$Z = Y + \tau \frac{dY}{dt}, \quad (1)$$

where τ is the relaxation constant of the electrode. Integration of the expression yields

$$Y = Z(1 - e^{-t/\tau}) + Y0, \quad (2)$$

where $Y0$ is the reading of Y at $t = 0$ and τ is the time it takes to reduce the error in electrode reading (Z-Y) to a value of (Z-Y)/e or ~37%. The value of τ was determined for each electrode in each set of experiments by recording the signals following an abrupt change in concentration of the measured species using the flow cell as described above. The observed changes in electrode signals were fitted by computer to the expression in Eq. 2. To determine a true rate of change of concentration from the observed electrode readings, the derivative of Eq. 1 with respect to time is needed.

$$\frac{dZ}{dt} = \frac{dY}{dt} + \tau \frac{d^2Y}{dt^2}. \quad (3)$$

Therefore, in addition to τ for each electrode both dY/dt and d^2Y/dt^2 must be determined as functions of time.

A typical electrode response curve for the O_2 electrode following the initiation of a respiratory pulse is shown by the solid sigmoidal curve in the top panel (Fig. 1). From the shape of the curve and the fact that the electrode response itself follows an exponential law, it seemed reasonable to try to fit the data collected from zero time to a two-exponential function. In using this approach, data were collected from 6 to 10 s just prior to opening the photographic shutter to initiate respiration. These

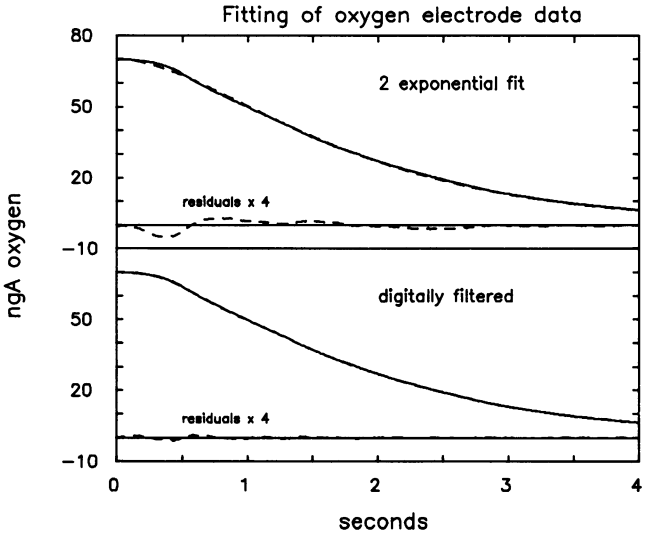

FIGURE 1 Fitting of O_2 electrode data. At zero time a photographic shutter was opened to initiate respiration in a mitochondrial suspension (18 mg protein in 6 ml) containing 200 mM sucrose,1.5 mM HEPES, 50 mM KCl, 2 μM rotenone, 18 μg oligomycin, 90 μg NEM, 2.2 ng valinomycin, 5 mM succinate and 60 to 120 ngA O, under an atmosphere of 100% carbon monoxide. Data was collected at the rate of 100 electrode readings per s. *Top* panel: The raw data are shown as a solid line. The fitting to a two-exponential function was done in two steps. First to eliminate uncertainty of the zero time value because of noise, six seconds of dark data just prior to opening the shutter were fit to a straight line function. Using the fitted zero value as a constraint, the data collected during the pulse were fit to the expression $Y = A1e^{-t/\tau_1} + A2e^{-t/\tau_2} + A0$ to obtain the dashed line drawn superimposed on the raw data. The residuals between the fitted and raw curves, multiplied by 4 are also shown. *Bottom* half: The raw electrode data (solid line) were passed five times through a cascading digital filter as described in the text. The filtered data (dashed line) are shown superimposed on the raw data. The residuals × 4 are also shown.

"dark data" correspond to a very slow electron flow and H^+ ejection, since in theory, competitive inhibition of O_2 and CO binding is never complete in the presence of even very low amounts of O_2. From the fact that illumination causes an immediate, sharp, and pronounced rise in both dH^+/dt and dO/dt (c.f. Fig. 7) and the observation of high early values for H^+/O ratios, we believe that the dark respiration had a negligible effect on the system. If any effect was exerted it would be in the direction of lowering early H^+/O ratios because of the formation of some level of $\Delta\tilde{\mu}_{H^+}$ prior to illumination. Therefore, the measured values seen here may be considered as possibly underestimates. The dark data were fit to straight lines to fix the values of the electrode readings and thus the O_2 and H^+ concentrations at zero time. This value was used as a constraint in the fitting process. A fitted two-exponential curve is shown as a dashed line superimposed on the curve of raw data shown in Fig. 1, top panel. The fit from 1 to 4 s is very good and the small deviations seen from zero to 1 s appear to be negligible. However, the residuals (multiplied by 4 for the illustration) reveal marked discrepancies in the critical early record of the pulse. It must be realized that in the current approach the H^+/O ratio is determined and updated from every 0.01 s ratio of dH^+/dt and dO/dt. Therefore, errors in early time values of the two slopes can translate into significant errors when one slope is divided by the other. The problem is compounded by the fact that errors in the first derivative are greatly magnified in the second derivative which is used to correct the observed rates to true rates using Eq. 3. Examination of all data sets by the two exponential fitting procedure revealed a systematic error of the kind illustrated by the residuals in this figure. It seems that the use of the two exponential mathematical model imposes an unreal condition that does not properly account for the early data of the experiment. Therefore, a technique of data analysis was developed that did not rely on adherance to a particular mathematical model. The simplest and most direct technique would be to determine empirically the observed first and second derivatives of electrode changes and use these according to Eq. 3 to determine true dH^+/dt and dO/dt and consequently H^+/O ratio as a function of time. The practical impossibility of this direct approach is realized when one considers that the first derivative (per s rate) determined from a 0.01 s time interval requires multiplication by 100 and that the computation of the rate of change of the first derivative involves another factor of 100. Any noise in the data, even that lasting only 0.01 s, will be greatly magnified in the second derivative and then, after multiplying by τ, added to the raw slope to obtain the true first derivative. It became possible to

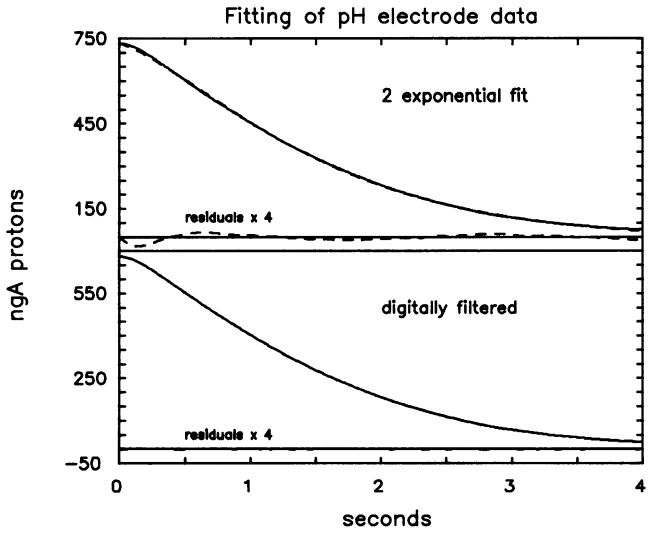

FIGURE 2 Fitting of pH electrode data. The explanation regarding the O_2 electrode data in Fig. 1 applies to the treatment of the pH electrode data shown here except that a four-pass rather than a five-pass filtration was applied.

use the direct or empirical approach only after a very powerful digital filter was designed that could greatly diminish noises of frequencies different from that of the biological and system responses. The filter employs a multipass cascading process and is separately described (Appendix). An illustration of the fidelity of this procedure is shown in Fig. 1, bottom panel with the raw data shown as a solid curve and the filtered data superimposed with a dashed line. The residuals multiplied by four are also shown to document the close correspondence of the raw and filtered data. Although the pH data when fit by the two exponential function appear at first glance to represent the raw data with high fidelity (Fig. 2, *top*) the residuals show essentially the same kind of deviations as seen with the O_2 data (c.f. Fig. 1, *top*). The digitally filtered pH data, on the other hand, do not show any discrepancy (Fig. 2, bottom). As was already mentioned, corrections for relaxation times of the electrodes employ the second derivative which amplifies noise several thousand fold. A clear demonstration of the power of the filters used here is shown in Fig. 3. The top panel shows the second derivative determined empirically from the raw O_2 electrode trace. This curve also illustrates the extreme sensitivity of the membraneless fast-responding O_2 electrode to motion, as evidenced by the apparent oscillation rate of 25 H, which corresponds to the stirring rate of the magnetic bar as determined with a stroboscope. The central curve in the top panel is the same data after digital filtering. The pH electrode does not show the motion artifact of the O_2 electrode, but it is seen that there is a definite noise pattern in the raw data that is markedly reduced by the digital filtration procedure.

RESULTS

Indications of an Early Burst in H^+/O Ratio

Fig. 4 shows the determination of τ or relaxation constant for the O_2 and pH electrodes. This procedure was performed in multiplicate for all experimental series. The upper panel shows both the raw trace from the O_2 electrode and the fitted curve using Eq. 2. Tau (τ) in this case was found to be 0.19 s. The lower panel shows the raw trace from the pH electrode and the fitted curve using Eq. 2. Tau was determined to be 0.23 s. Using the digital filtration procedure and direct determination of H^+/O ratios from the values of dH^+/dt and dO/dt determined every 0.01 s and corrected for electrode response delays, typical records of four experiments are shown in Fig. 5. The solid curves show the response time-corrected ratios and the dashed lines show the ratios obtained from the filtered data uncorrected for response times. With the fast responding electrodes used in this work, the two curves tend to merge after ~1 s. All curves show an early burst in H^+/O ratio that is damped out within 0.3 s in the corrected curves but lingers to between 0.5 and 1 s in the uncorrected curves. The traces also show a noise pattern that is more pronounced in the corrected curves and becomes more evident after the early burst. This is understandable because although the filter is very effective, a small amount of noise does pass. This noise is greatly magnified during the process of correcting for response times as discussed in the experimental section. As both dH^+/dt and dO/dt decrease because of respiratory control, the ratio of the two becomes more sensitive to noise especially as dO/dt approaches zero. The true curve is easily seen as the average running through the regular noise pattern. All curves are in agreement on the existence of an early burst in H^+/O ratio and in a value of 4 or greater at 1 s.

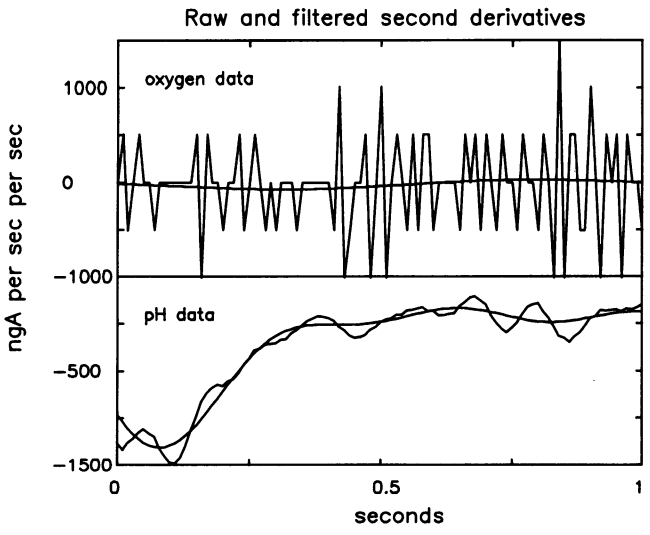

FIGURE 3 Raw and filtered second derivatives. Second derivatives were taken directly from either the raw electrode readings or from the digitally filtered data. The number of filter passes was five for the O_2 data and four for the pH data. The curves with many oscillations in both upper and lower panels represent second derivatives obtained from the raw data and the central curves in the two panels represent the second derivative obtained from the filtered data.

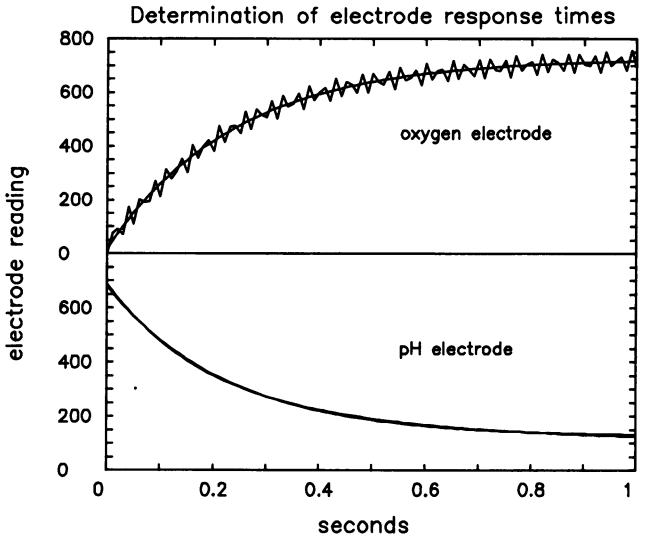

FIGURE 4 Determination of electrode response times (τ). The electrodes were subjected to rapid changes in concentration of the ion measured by using the flow cell described in the experimental section. The raw electrode data (readings in arbitrary units) were fit to Eq. 2 in the text to obtain the relaxation constant, τ, for each electrode. Each panel shows both the raw data and the fitted curve. The value of τ obtained in the experiment shown in the top panel was 0.24 s. If the raw data were first filtered with five passes through the digital filter, the value of τ obtained was 0.25 s. The value of τ obtained in the experiment shown in the bottom panel was 0.23 s.

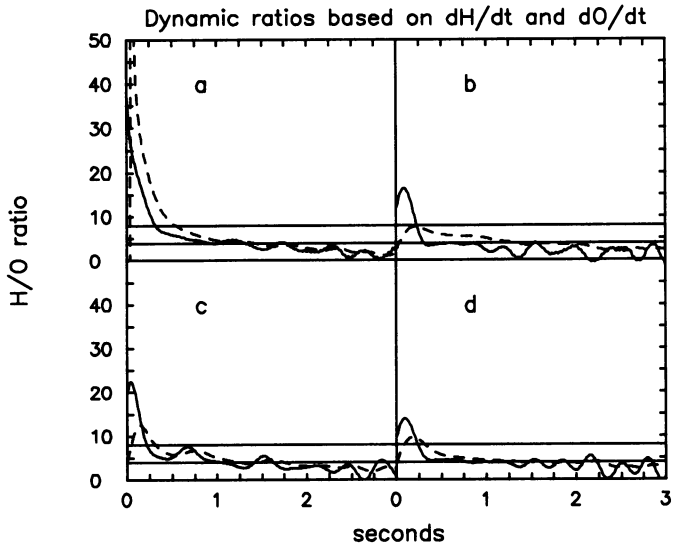

FIGURE 5 Dynamic ratios based on dH^+/dt and dO/dt. Data collected during a respiratory pulse, initiated upon illumination of a mitochondrial suspension (described in Fig. 1) with succinate as substrate were collected at a rate of 100 readings per s per electrode and digitally filtered using five passes through the filter for O_2 data and four for pH data. First and second derivatives were obtained from the filtered data as described in the text. Relaxation constants ($-\tau$) were measured for each electrode as shown in Fig. 4. The electrode data were corrected for response times using Eq. 2 in the text. H^+/O ratios were determined by the ratio of dH^+/dt to dO/dt for each 0.01 s increment of time. These curves are shown as solid lines. The same procedure but omitting corrections for response times of the electrodes was used to obtain the uncorrected or apparent H^+/O ratios which are shown as dashed lines in the figure. Panels *a*, *b*, *c*, and *d* show experiments performed with mitochondria from series H1, H2, N2, and N3, respectively, as shown in Table I and described in the text.

Attempts to Explain the Early Burst as an Artifact of Measurement

A burst phenomenon occurring within the first 300 ms could not have been seen by earlier methods used to study H^+/O stoichiometries. If the phenomenon is the result of physiological processes, it is important to understand it in molecular terms. However, since this is the first indication of such a phenomenon, and its observation is dependent on new procedures, considerable effort was expended in trying to find alternative (i.e., nonphysiological) explanations.

Possible Delay in Measurement of Initial dO/dt Because of Occluded O_2 Pools

A Zone of Diminished O_2 Concentration Around the Tip of the O_2 Electrode or Within its Sintered Glass Coating. The O_2 electrode consumes O_2 during the measurement and a zone of diminished O_2 tension is maintained close to the sensitive electrode tip. Part of the relaxation time of the electrode is due to the diffusion of O_2 from the bulk solution across this zone to the platinum electrode. The size of this zone can be influenced by the shear force of the stirred liquid flowing across the electrode tip. By the use of a stroboscope to determine the oscillation rate of the liquid and considering the geometry of the electrode position with respect to the magnetic stirring bar, the rate of flow of solution past the tip was calculated. This flow rate was duplicated in the determination of τ in the flow cell so that this kind of artifact could be diminished or eliminated.

Another possible location for a sequestered O_2 pool may be in the volume of liquid trapped in the sintered glass coating of the O_2 electrode. Such a pool might delay the sensing of an initial decrease of O_2 in the bulk phase. This possibility is quickly dismissed by a simple calculation. The average duration of the burst phenomenon was 0.3 s and involved ~120 nmol H^+ and 10.4 nmol O per 18 mg of protein used in the experiment. If an underlying mechanistic H^+/O ratio is assumed and if it is further assumed that no retardation of H^+ translocation occurred during the whole burst period, then at a ratio of 4, ~30 nmol O should have been consumed, and at a ratio of 8, ~15 nmol O should have disappeared. The short-fall in O_2 amounts to 4.6 to 19.6 nmol. At the concentration of O_2 used in these experiments (~8 μM), this represents 0.29 to 1.2 ml solution. With the area of the O_2 electrode (~0.0314 cm^2), this would require a thickness of 9.2 to 38 cm assuming the sintered glass itself occupied no volume, whereas the actual thickness of the sintered glass coating is of the order of microns.

Intramitochondrial O_2 Pools. A sequestered pool of O_2 inside the mitochondria could also lead to initial kinetic artifacts yielding values of dO/dt not representative of O_2 uptake rates of the mitochondria. For example, the internal volume of the mitochondria may provide the O_2 for the initial proton burst that is not accounted for in

terms of disappearance of O_2 from the bulk phase sampled by the O_2 electrode. This possibility was easily checked as follows. The mitochondrial internal volume is ~1 μl/mg of protein. The assumption was made that this space was in equilibrium with the O_2 of the bulk phase at zero time and that this O_2 pool was totally consumed the instant the respiratory pulse was started. A cumulative H^+/O ratio was calculated at every time point using the bulk amount of H^+ appearing in the external phase and the bulk amount of O_2 disappearing plus the total possible internal O_2 pool. Fig. 6 shows the H^+/O ratios computed in this manner for the same four experiments shown in Fig. 5. Although the addition of the maximum amount of O_2 that could have been contained in the internal pool diminished the magnitude of the initial burst and understandably pushed the peak to a later point in time, the burst was not accounted for by such a sequestered pool. In fact, including the initial H^+ burst in the cumulative bulk ratio, maintained the H^+ ratio above 4 throughout the first 3 s of the respiratory pulse.

A sequestration of the O_2 pool that is responsible for the burst in either the periplasmic space or in the external membrane is eliminated by the fact that mitoplasts, which are missing these two compartments show the same burst behavior as intact mitochondria (to be reported separately). While it is true that O_2 is ~4 times more soluble in paraffin oil than in aqueous buffer, the hydrophobic volume of the inner membrane is so small relative to the matrix volume of the mitochondria, that insufficient O_2 could be held in this compartment to account for the burst.

Therefore, neither an internal mitochondrial pool of O_2 nor a pool of O_2 contained in the sintered glass covering of the electrode can account for the burst phenomenon.

Unstirred Layers Around the Mitochondria. A more subtle possibility for the location of a sequestered pool of O_2 is in an unstirred layer surrounding each mitochondrion. Because the diffusion constant for H^+ (D_H) is five times greater than that for O_2 (D_0) in aqueous media, it could be imagined that O_2 from this layer is consumed before, O_2 begins to leave the bulk phase and that the H^+ released, rapidly traverses the layer to be sensed by the pH electrode. The characteristic delay time for diffusion of O_2 through such a layer is given by the Fick expression (7)

$$\tau = \frac{\delta^2}{D},$$

where τ is the delay time in s, δ is the thickness of the layer in cm and D is the diffusion constant for O_2 ($\sim 1 \times 10^{-5}$/cm^2 s). The expected time for the beginning of a loss of O_2 from the bulk phase can be approximated by τ/π. The radius of the matrix space of a mitochondrion can be calculated from the facts that a mg of mitochondria protein represents ~2 mg dry weight, which at an average of 1.1×10^{-13} g per mitochondrion translates into $\sim 1.82 \times 10^{10}$ mitochondria. With a sucrose impermeable space of 1 μl, each mitochondrion has a matrix radius of $\sim 0.24 \times 10^{-4}$ cm. If the average radius of an intact mitochondrion is

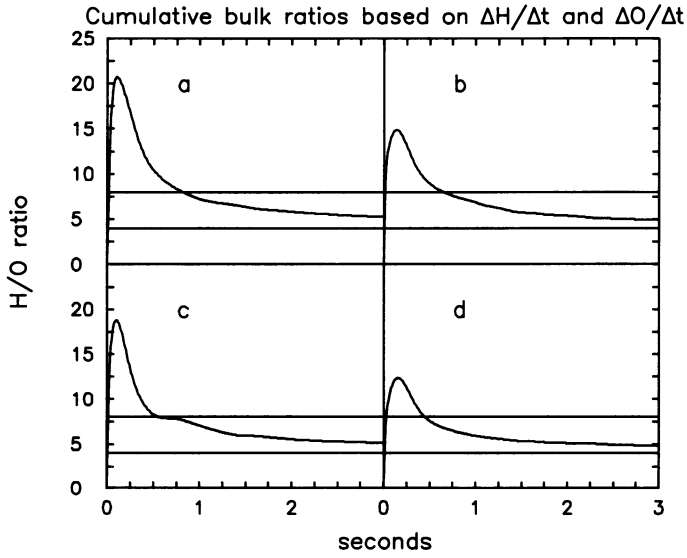

FIGURE 6 Cumulative bulk ratios based on $\Delta H^+/\Delta t$ and $\Delta 0/\Delta t$. Electrode data were collected, digitally filtered, and corrected for response times as described in Fig. 5 and the text. The H^+/O ratio at each time point was computed as follows. The total amount of protons appearing in the external medium was divided by the total amount of O_2 disappearing from the external medium plus the total amount of O_2 that could have been inside the mitochondria at zero time. The internal pool was estimated assuming complete equilibration with the external pool at zero time and an internal volume of 1 μl/mg protein. With 18 mg protein/6 ml used in the current experiments, the internal pool would represent 0.003 times the total O_2 content of the flask at zero time. Panels *a*, *b*, *c*, and *d* are the same as described in Fig. 5.

taken as 1 μl and the periplasmic space considered as the unstirred layer, the expected delay time for a loss of O_2 from the bulk phase would be ~0.17 ms. If all of the volume of the mitochondrial suspension were considered to be unstirred and distributed equally to all of the mitochondria, this time would be increased to ~0.66 ms. To account for the observed burst phenomenon which lasted ~300 ms, an amount of additional unstirred volume would be required to increase the thickness of the unstirred layer by ~20 times. Experimental verification of this conclusion is available. During the time that O_2 is being consumed from an unstirred layer, there should be no disappearance of O_2 from the bulk phase. Therefore, if an unstirred layer were responsible for the 300 ms burst phenomenon, the appearance of O_2 consumption should have been preceded by a period of up to 300 ms with little or no loss of O_2 from the bulk phase. In fact, all of the records show an immediate onset of O_2 consumption the instant that the suspension is illuminated and acidification is observed. Therefore, unstirred layer phenomena cannot account for the burst.

Artifacts Due to Electrode Idiosyncracies or Correction Procedures for Electrode Response

Experimental Test of Initial Electrode Behaviors. In applying corrections for the relaxation characteristics of the electrodes, it has been assumed and demonstrated (c.f. Fig. 4) that both electrodes essentially obey a single exponential law. It may be wondered whether each electrode may deviate subtly in its initial response in such a way as to cause an apparent burst in H^+/O ratio where none exists. To test this possibility, data were taken from the flow-cell, where both electrodes were simultaneously subjected to a step change in concentration for the ion measured. There should be no initial burst in H^+/O ratio under these circumstances. Such data from a large number of flow cell experiments were analyzed. If the correction procedures are adequate, it is to be expected that a step change in H^+/O ratio should be seen. Analysis of these experiments showed that in all cases, the achievement of the new stable level of H^+/O ratio was preceded by a period of 50 to 100 ms of a gradual rise period (data not shown). This was true for both the dynamic ratio determined from 10 ms values of dH^+/dt and dO/dt and for the bulk ratio determined from ΔH^+ and $\Delta 0$. Therefore, if the initial conditions in the flow cell represent the situation when the illumination of the stirred suspensions starts the processes of O_2 uptake and H^+ extrusion, the magnitude of the burst may have been underestimated, but the burst could not have been artifactually caused by deviations in electrode behavior.

It will be shown below (Fig. 9) that the response time correction procedure cannot introduce a burst in a truly one-exponential process that is being followed by the electrode.

Independent Estimates of τ From Initial Delays in Measurements and Dependence of Existence of Burst Phenomenon on Value of τ Used. It is important to note that because of the short lifetime of the early burst, its magnitude depends on the corrections we have applied for the relaxation times of the electrodes. Although the flow cell does present the electrode with an abrupt change of concentration for its particular ion, it must be recognized that the actual experiment takes place in another vessel. There are two ways in which the burst could have been unduly exaggerated. One is that the pH electrode in the experimental flask is much faster than the ~0.2 s time constant we have measured in the flow cell and the other is that the O_2 electrode is really much slower than the ~0.2 s that we have measured. Because of the time constant in the electronic filter of the electronics system, no signal faster than $\tau = 0.05$ will be passed. This is the absolute fastest response the pH electrode could have produced. Using this value of 0.05 s in the computation did not remove the burst phenomenon from the data. Fortunately, there is an independent indication of the actual time constant for the electrode in situ at the time of the experiment. An instantaneously responding electrode following an exponential change in concentration such as seems to occur during the respiratory pulse will produce a one-exponential curve. A response delay in the electrode shows up as an additional exponential in the beginning of the curve. Fig. 2 very clearly shows the initial exponential delay in the pH electrode's response to initiation of the respiratory pulse. The computer-fitted τ for this initial exponential in the two-exponential curve fits was 0.26 ± 0.05 s for the series H1 compared to the flow cell's measured value of 0.19 s, and 0.38 ±0.05 s for the series N2 compared with 0.20 s found in the flow cell. It therefore seems more likely that the response of the electrode in the actual experiment may have been somewhat slower than in the flow cell but the possibility of an instantaneous response seems to be eliminated. In the case of the O_2 electrode, a τ of 0.59 ±0.06 s was measured for the first exponential in the two exponential fits of series H1 compared to the flow cell's value of 0.23 s, and 0.37 ±0.06 s was measured in the two exponential fits for series N2 compared with the flow cells measured value of 0.15 s. The initial rate of change of O_2 upon initiation of the pulse was found to be slower than that for the pH as shown in Fig. 8 (discussed below) using corrected data and this seems to be a characteristic of the phenomenon studied here. If true, this effect would account for the higher values of τ obtained in the two exponential fitting of the experimental data compared to the direct measurements in the flow cell. At any rate, using the slower time constants found in the two exponential fittings still did not eliminate the burst phenomenon.

Influence of Electron and Digital Filtration Procedures on Existence and Magnitude of H^+/O Ratio Burst Phenomenon. The possibility was considered that the data filtering procedures may have contributed to the appearance of the burst phenomenon. Prior to using these procedures it was determined that the residuals between the raw and filtered data did not show any bias introduced by the filtering procedures. Considering, however, that a five-pass process was used for the O_2 data and a four-pass procedure for the pH data, distortions due to the Gibbs phenomenon may have been introduced (see reference 1 in Appendix).

To insure that the filters were not introducing sufficient artifact to create a burst in the H^+/O ratio, a study was done on artifactual data consisting of a steady equilibrium followed by an exponential decay to another equilibrium, i.e.,

$$z(t) = 1 \text{ for } t < 0$$
$$= e^{-t/\tau_1} \text{ for } t \geq 0.$$

The "true" signal $z(t)$ was then subjected to a theoretical electrode delay time of $\sim 2 = 0.25$ s so that the "observed" signal was

$$y(t) = \left[\frac{e^{-t/\tau_1}}{\tau_2} - \frac{e^{-t/\tau_2}}{\tau_1}\right] \Big/ \left[\frac{1}{\tau_2} - \frac{1}{\tau_1}\right] \text{ for } t \geq 0.$$
$$= 1 \text{ for } t < 0.$$

The question was: how much error might be caused by filtering, differentiating, and correcting $y(t)$ to approximate the derivative $z(t)$. Trials were run for $\tau_1 = 0.5$ s or slower, as 0.5 is faster than any observed process in the real data. The results indicate that a worst case magnification of H^+/O ratio in the first 50 ms was 25%, not nearly enough to account for the observed burst. Furthermore, this worst case arises only when $\tau_1 = 0.5$ in both H^+ and O_2 curves, a situation not approached by the real data. Because the raw O_2 curves exhibit a considerably slower startup than the raw H^+ curves, it is far more likely that the H^+ derivative at startup is damped more by its digital

TABLE I
SUMMARY OF RESULTS COMPUTED FROM 0.01 SECOND VALUES OF dH^+/dt AND dO/dt

	Oxygen	Peak H^+/O		1/2 Peak H^+/O	End of burst	H^+/O Value			
		Value	Time	Time	Time	Corrected		Uncorrected	
						0.5 s	1.0 s	0.5 s	1.0 s
	ngA/ml		*s*	*s*	*s*				
N1	16.5 ± 1.5	13.6 ± 1.6	0–0.05	0.35 ± 0.03	0.35 ± 0.04	5.8 ± 0.4	4.6 ± 0.3	7.0 ± 0.4	4.9 ± 0.3
	(5)	(6)		(4)	(4)	(4)	(6)	(6)	(6)
N2	12.5 ± 1.1	16.6 ± 2.9	"	0.23 ± 0.03	0.24 ± 0.01	5.8 ± 0.3	4.7 ± 0.17	6.0 ± 0.22	4.9 ± 0.10
	(5)	(5)		(5)	(5)	(5)	(5)	(5)	(5)
N3	11.0 ± 0.4	12.8 ± 1.3	"	0.26 ± 0.02	0.28 ± 0.02	4.2 ± 0.2	3.2 ± 0.1	5.0 ± 0.2	3.9 ± 0.14
	(12)	(10)		(10)	(12)	(12)	(12)	(12)	(12)
H1	15.6 ± 0.8	23 ± 3.2	"	0.24 ± 0.03	0.33 ± 0.02	5.9 ± 0.2	4.2 ± 0.2	7.8 ± 0.3	4.9 ± 0.2
	(14)	(14)		(14)	(13)	(14)	(14)	(14)	(14)
H2	9.9 ± 0.6	38 ± 9.2	"	0.16 ± 0.02	0.27 ± 0.01	3.2 ± 0.2	2.5 ± 0.1	5.3 ± 0.2	4.2 ± 0.2
	(9)	(9)		(9)	(9)	(9)	(9)	(9)	(9)

COMPUTED FROM ACCUMULATED BULK ΔH AND ΔO CORRECTED FOR INTERNAL OXYGEN

	Peak H^+/O		Total Change During Burst (ngA/mg Protein)		H^+/O Value Corrected		
	Value	Time	H^+	0	1.0 s	2.0 s	3.0 s
		s					
N1	8.8 ± 1.1	0.26 ± 0.05	5.0 ± 0.5	0.62 ± 0.08	5.9 ± 0.2	5.2 ± 0.2	5.0 ± 0.3
	(6)	(4)	(5)	(5)	(6)	(6)	(6)
N2	14.0 ± 1.9	0.12 ± 0.01	5.2 ± 0.2	0.49 ± 0.06	6.5 ± 0.4	5.5 ± 0.3	5.0 ± 0.2
	(5)	(5)	(5)	(5)	(5)	(4)	(4)
N3	13.7 ± 2.1	0.13 ± 0.01	4.5 ± 0.3	0.51 ± 0.04	5.1 ± 0.2	4.4 ± 0.1	4.1 ± 0.1
	(12)	(12)	(12)	(12)	(12)	(12)	(12)
H1	17.7 ± 1.4	0.14 ± 0.01	7.3 ± 0.5	0.61 ± 0.05	7.0 ± 0.1	5.6 ± 0.2	5.1 ± 0.2
	(14)	(14)	(13)	(13)	(14)	(14)	(14)
H2	28.7 ± 5.6	0.10 ± 0.01	7.1 ± 0.5	0.49 ± 0.06	6.1 ± 0.3	4.9 ± 0.2	4.5 ± 0.2
	(9)	(9)	(9)	(9)	(9)	(9)	(9)

The experimental procedure is described in detail in the Experimental Section. The mitochondrial supension is described there and in Fig. 1. N1, N2, and N3 refer to preparations of mitochondria made on three difference days at NIH. H1 and H2 refer to preparations of mitochondria made on two different days at Johns Hopkins Medical School. The relaxation time constants, in seconds, used to correct for electrode response times of the pH electrode and the O_2 electrode in the series N1, N2, N3, H1, and H2 respectively, were 0.17 and 0.13; 0.20 and 0.14; 0.28 and 0.22; 0.19 and 0.23; and 0.46 and 0.24.

filter than the O_2 derivative is. Consequently, the H^+/O burst is possibly underestimated by the filtered data, by as much as 35%. For these trials to be valid, it is not necessary for the real data to be exponential. It is sufficient that the data can be approximated by $y(t)$ with appropriate τ's and scaling in the neighborhood of $t = 0$. We have also found the burst to be present when the raw data were both fit to two exponential models and no filtration process employed. Therefore, the 25% theoretical burst is to be used as a worst case estimate and not descriptive of the experiments.

Experimental Determination of Proton Extrusion and O_2 Uptake Rates During Succinate Oxidation

Table I presents a composite summary of the experimental data. The top half presents information on H^+/O ratios determined from 0.01 s increments of electrode response corrected values for dH^+/dt and dO/dt. The bottom half uses the corrected values for H^+ and O concentrations as functions of time to determine bulk changes. The H^+/O ratios in this case were computed by dividing the total amount of H^+ appearing in the external medium by the total amount of O_2 disappearing plus the maximum estimate for the total amount of O_2 contained in the mitochondrial matrix at zero time for each time point indicated. Internal volume was taken as 1 μl/mg of protein which for the 18 mg of protein used per 6 ml incubation volume represents an amount of 18/6,000 or 0.003 times the starting O_2 content of the flask. The experiments involved separate preparations of mitochondria from five rats. Three preparations were made at NIH (N1, N2, and N3) and two at Johns Hopkins (H1 and H2). A total of 46 experiments are presented covering a range of zero time O_2 concentrations of 9.9 to 16.5 ngA O per ml or from 2 to 3.5% the saturation level of buffer in equilibrium with air. Successive pulses performed on the same mitochondrial suspension after waiting for full resorption of translocated protons produced the same overall behavior as seen in the initial pulse. All experiments showed an initial burst in H^+/O ratios that reached a peak prior to 50 ms. When corrections were made for electrode response times, the burst was seen to last only ~0.3 s. When no corrections were made, the apparent decay was slower, and values at 0.5 and 1 s were higher than obtained with the corrected data. With slower electrodes than used here this effect could be more pronounced. In a few cases, the initial burst was either atypically very short leading to H^+/O values out of line with the general trend or rather diffuse in which case 0.5 s values were effected. In these cases, the atypical values were eliminated from the averages. The two lowest O_2 concentrations (11 and 9.9 ngA 0/ml) were associated with noticeably lower values for corrected dynamic H^+/O ratios at 0.5 and 1 s. The other estimates of H^+/O ratio appear to be less affected, if at all, at these O_2 levels.

Fig. 7 shows some important controls. In the absence of added substrate (*left* panel) opening of the photographic shutter to illuminate the mitochondrial suspension did not cause a change in either the O_2 electrode trace or the pH electrode trace. When succinate was present (*middle*

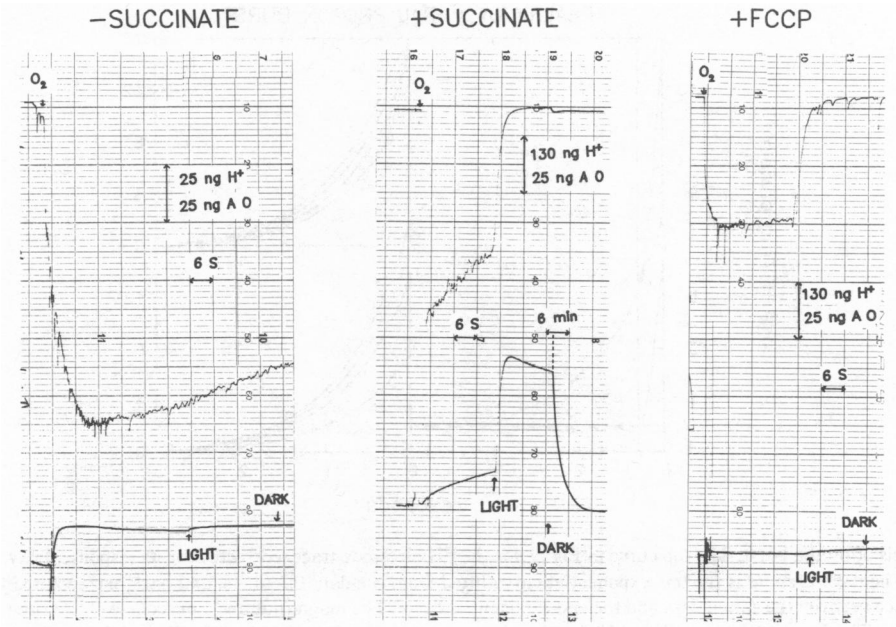

FIGURE 7 Control experiments. The mitochondrial suspension is the same as described in Fig. 1. Arrows marked with O_2, LIGHT, and DARK denote times at which air-saturated buffer was added, illumination of the suspension started, and illumination stopped. In the experiment shown in the left panel, succinate and 10 μM FCCP were both present. Chart speed was 1 cm/6 s except for the period shown to the right of the vertical dashed line in the center panel, where the slow resportion of extruded protons was followed. Chart speed during this period was 1 cm/6 min.

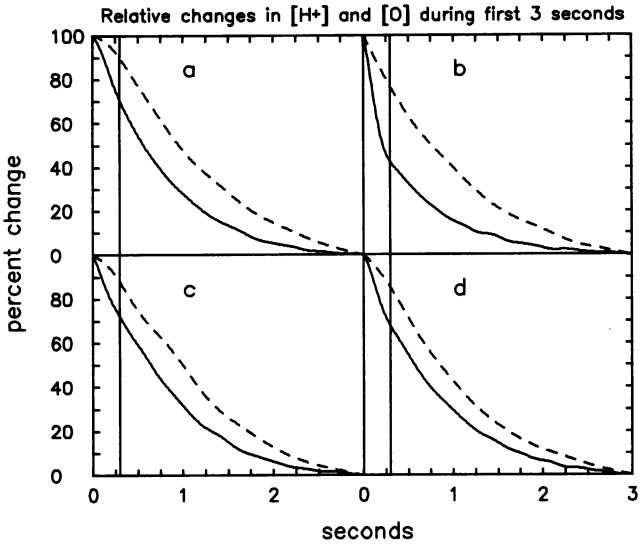

FIGURE 8 Relative changes in $[H^+]$ and [O] during first 3 s of a respiratory pulse. Panels *a*, *b*, *c*, and *d* represent experiments as described in Fig. 5. The digitally filtered electrode data, representative of O_2 and H^+ concentrations, corrected for response times, were normalized to 100% of the change occurring in the first 3 s of the respiratory pulse. H^+ data are shown as solid lines and O_2 data as dashed lines. Vertical lines are drawn at 0.3 s to mark the approximate end of the initial burst in H^+/O ratios. The relaxation time constants used for correcting electrode readings are given in the legend to Table I.

panel) there was a slow rate of carbon monoxide-resistant respiration (before illumination) and a large burst of rapid O_2 uptake and proton extrusion upon illumination. Following consumption of all of the O_2 there was a slow return of all of the extruded protons so that the initial reading of the pH electrode is re-established. In the presence of succinate and the protonophore 10 μM FCCP, the uptake of O_2 upon illumination was not accompanied by acidification of the medium, as was to be expected.

Attention was focused on the initial data obtained from of the pH and O_2 electrodes to determine whether the burst involved an actual "extra" release of protons or simply an initial delay in O_2 uptake. Fig. 8 shows the individual corrected electrode responses during the first 3 s, normalized to 100% for each electrode. The traces show that in the period of the burst (~300 ms), there was both an initial delay in O_2 uptake and an initial enhanced rate of H^+ release, the latter being most evident in Fig. 8 *b*. The phenomenon of enhanced H^+ release, is further illustrated in Fig. 9. Another pulse from the same series shown in Fig. 8 *b* is shown in Fig. 9 *a*. The upper solid line is the corrected pH electrode trace scaled in units of ngA H^+/mg protein. The dashed line is the extrapolation of the one exponential portion of the curve, fit from 0.3 to 3 s. The difference between these two curves is shown in the bottom portion of the panel. The magnitude and time course of the burst phenomenon is evident. The effect of the correction procedure on the response delay of the electrode is shown in Fig. 9 *b*. The uncorrected curve is at the top and the results of increasing amounts of correction are shown in the three

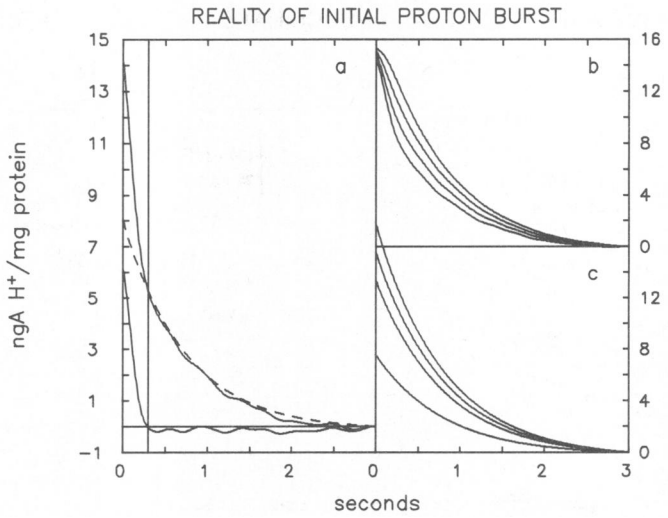

FIGURE 9 Analysis of proton burst. The top curve in Fig. 9 *a* is the pH electrode trace, corrected for its response delay, for the first 3 s of a respiratory pulse. The dashed curve is the one-exponential curve fitted from the data 0.3 to 3 s, and back extrapolated to zero. The bottom curve is the difference between the actual data and the one-exponential curve. The magnitude and time course of the burst is seen. The vertical line is drawn at 0.3 s. The *Y* axis shows the electrode signal scaled to ngA H^+/mg protein. Acidification of the medium causes a decrease in signal. The effect of the correction for response time is shown in Fig. 9 *b*. The top trace is the uncorrected raw data and the bottom trace is the fully corrected data. Two intermediate levels of correction are also shown. The result of the correction is the removal of the initial delay phase seen in the top curve. The effects of applying corrections for response time to a single exponential curve are shown in Fig. 9 *c*. The top curve is a one exponential curve obtained from a fit of the raw data from 0.3 to 3 s. The extents of correction are the same as were applied to the curves shown in Fig. 9 *b*. These three panels show that the apparent proton burst is inherent and not due to the correction procedures.

lower curves, the lowest representing the fully corrected case. It is seen that the correction procedure removes the initial delay that is seen in the uncorrected curve. One may be concerned that the correction process itself may introduce an "apparent" burst where none exists. This is shown not to be the case in Fig. 9 *c*. The top curve is a one exponential curve fitted to the uncorrected pH trace from 0.3 to 3 s and extended to zero. The same degrees of correction used for Fig. 9 *b* were applied to the curve and are shown in the three lower traces in Fig. 9 *c*. All curves in Fig. 9 *c* are strictly one exponential and no spurious more rapid phase has been introduced in the beginning of the curves. This result is to be expected because the correction procedure corrects the inherent time-constant process and does not introduce a new exponential phase.

Analysis of Data Obtained After 0.8 s. In the "second generation" approach of Costa et al., data obtained from the fast-responding O_2 and pH electrodes after 0.8 s were expressed as rate increments, fit to one exponential functions in a Guggenheim plot of rate vs. time, and zero time values were obtained by extrapolation. The data obtained in our experiments from 0.8 s and beyond can be treated in a similar fashion. Fig. 10 shows typical raw data from the two electrodes at 0.2 s intervals, in plots of amount vs. *t*. Both curves can be fit by single exponential expressions. When the data of Fig. 10 is re-expressed in semi-log Guggenheim plots, the one exponential linear curves appear to be a true representations of the data (Fig. 11). Experimental data from 31 experiments in the series N1, N2, and H1 (c.f. Table 1) were treated in this way to obtain zero time values by extrapolation. The average value and the standard error of the mean for these experiments was 8.0 ±0.4.

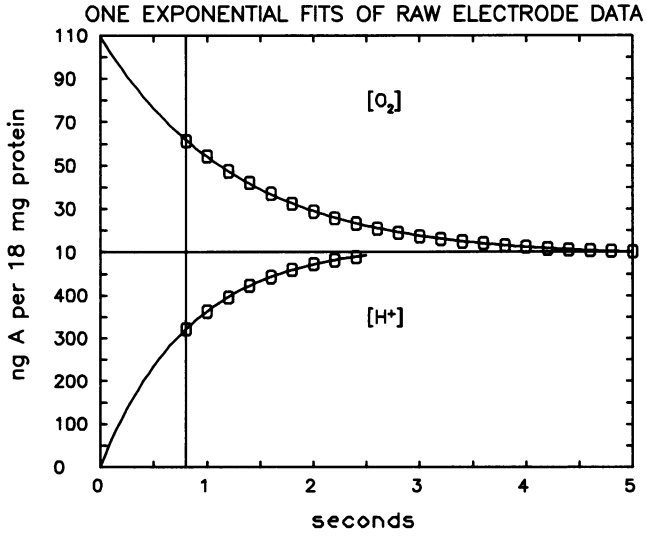

FIGURE 10 Representative raw electrode data from 0.8 to 5 s for the O_2 electrode (*top*) and from 0.8 to 2.4 s for the pH electrode (*bottom*). The solid lines are theoretical 1 exponential curves fit to the data shown at 0.2 s intervals (circles).

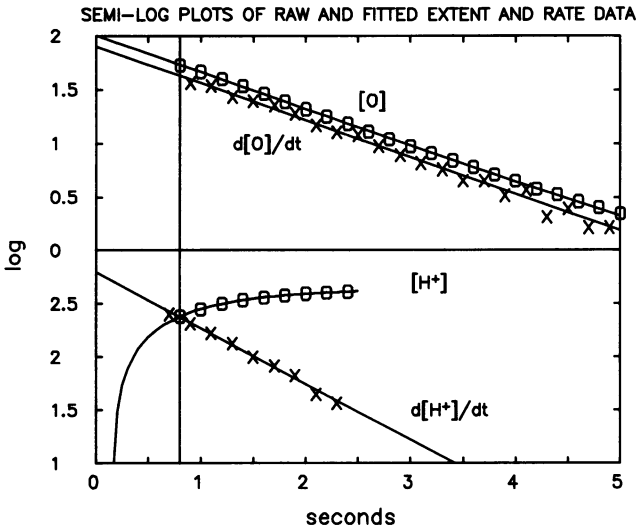

FIGURE 11 The data displayed in Fig. 10 are shown on semi-log plots here (circles) and after conversion to rates based on increments of the 0.2 s intervals. The parameters obtained in the one-exponential fits shown in Fig. 10 were used to draw the curves shown in this figure.

DISCUSSION

In the experiments reported in this paper, major improvements were introduced for the determination of initial and early values of H^+/O stoichiometries. These are:

(*a*) The mixing-time was essentially eliminated by the photolysis technique.

(*b*) A correction procedure for electrode relaxations based on experimental data was used.

(*c*) Noise was greatly reduced by a combination of electronic and digital techniques.

(*d*) Direct data collection by computer at 10-ms intervals eliminated recorder delays.

(*e*) Actual data collected from zero time onwards eliminated uncertainties due to extrapolation. Because of the several stages of electronic and digital filtering used, actual values of H^+/O ratio within the first 50 ms could, in the worst case, be overestimated by 25%. On the other hand, the small degree of dark respiration prior to the photolysis may tend to produce underestimates in the earliest ratios.

(*f*) Elimination of the assumption of, and dependence on a particular mathematical model for the data, such as a single exponential or even a combination of exponentials.

Using this new approach we have found a burst in H^+/O ratios that peaks prior to 50 ms with a value of ~20–30 and decays within 300 ms to a point where it is no longer evident. If corrections for electrode response times are not made, the last phase of the burst will still be evident from 0.5 to 1 s. We attach no significance to a particular value for H^+/O ratio within the range of 20–30 in the first 50 ms. The important observation is that some form of burst in this ratio, well above the expected values of 6 and 8, seems to occur. Considerable effort was spent in trying to find nonphysiological explanations of this phenomenon. Such considerations involved occluded O_2 pools, the proce-

dures used for determining electrode response times, the procedures used for correction of electrode delay, idiosyncrasies of electrode behavior, the use of analog and digital filters and Gibb's phenomena resulting from the separate digital filtration of the pH and O_2 data. None of these effects was able to account for the burst. When the individual electrode responses were examined it was found that the burst involved both an initially enhanced rate of acidification and an initial lag of O_2 uptake. In addition to consideration of nonphysiological explanations, it is worth noting that there are positive indications that the phenomenon is physiological.

The magnitude of the burst appears to depend on the preparation of the mitochondria. The 23 experiments performed with mitochondria prepared at Johns Hopkins produced significantly higher bursts than the 23 experiments using the mitochondria prepared at NIH. The reason for the higher H^+/O burst ratios found with the Johns Hopkins mitochondria was that greater amounts of protons were extruded rather than lesser amounts of O_2 uptake during the burst. The averages of all of the experiments performed with these mitochondria expressed per mg protein were 7.2 ±0.3 ngA H^+ extruded and 0.56 ±0.04 ngA O consumed during the burst. The averages for the NIH mitochondria were 4.8 ±0.2 ngA H^+ and 0.53 ±0.03 ngA O. Furthermore, when the five individual series are arranged in the order of increasing peak values for H^+/O ratio, there is a direct correlation with the amount of proton extrusion during the burst and not with the extent of O_2 consumption. The attempts at using a two exponential model for the data support the existence of the burst phenomenon in another way. It was found in all cases that the initial changes in both H^+ and O followed a course not accounted for by simply two exponentials. The maximum deviation of the fitted two exponential curves for both pH and O_2 occurred during the early burst phase time of the pulse and thereby indicate that some additional phenomenon is occurring during this time period. The initial phase of the O_2 trace showed a rate less than the maximum uptake whereas the initial rate of proton ejection was at a peak which decayed after ~0.3 s to a slower approximately monotonic rate of decrease. It is important to emphasize that the initial kinetics observed for O_2 consumption in these studies may be related to a particular state of cytochrome *c* oxidase imposed by the presence of CO and O_2. That this may be so is indicated by newer studies (8) with the reduced anaerobic enzyme suddenly confronted with a pulse of O_2, which showed that there is an initial rapid phase of O_2 uptake followed by a slower phase.

It was shown here that when data from 0.8 to several seconds were fitted to single exponential expressions and extrapolated back to zero, the calculated H^+/O ratio tended to cluster close to 8.0. However, in all extrapolation procedures there are uncertainties. First, there is no theoretical reason to expect that either O_2 uptake or H^+ release should necessarily adhere to single exponential kinetics. To the extent that these curves contain information about other processes, the zero time values obtained from single exponential extrapolations will be in error. That other processes are probably occurring is indicated by the fact that the residuals of the O_2 vs. t curve and the two exponential fitted curve show systematic deviations from the beginning of the reaction. Moreover, newer data indicate that the O_2 consumption kinetics may involve two or three kinetic phases (8). In the case of the $[H^+]$ vs. t kinetics, a H^+ leak occurs simultaneously with a H^+ translocation process. The H^+ leak itself may be biphasic if it is governed differently by $\Delta\psi$ and ΔpH. The electrode response may also introduce difficulties. The ability to fit either curve to a theoretical single exponential function does not remove these doubts, because a theoretical curve contructed from two exponentials can be fitted with a single exponential in a manner which is convincing to the eye, but resolvable by the computer. Moreover, zero time H^+/O values obtained by extrapolation of this curve varied with the portion of the curve used for fitting. An indication of the existence of more information in the $[H^+]$ vs. t curve than just that of a single exponential is that the kinetic constant in the exponential is always greater than that for the $[O_2]$ vs. t curve. Since H^+ extrusion follows from and requires O_2 uptake, the two curves should have the same exponential constant. The value of 8.0 obtained here for the H^+/O stoichiometry utilized $[H^+]$ vs. t data obtained from the period 0.8 to 2–3 s. The inclusion of data beyond 3 s tended to yield higher values, whereas restricting the range to <2 s tended to yield lower values. We believe that the precise H^+/O ratio at very early times is subject to re-evaluation by more sophisticated direct measurement techniques such as were used in this work, as well as in other studies yet to be reported (e.g., Hendler, Froehlich, and Bhatnagar; Beavis and Lehninger; Reynafarje and Lehninger). The application of the newer methods should provide data to confirm or modify the findings reported here.

APPENDIX

A Family of Filters

Given a data vector $\mathbf{x} = [x_i, i = 1 \text{ to } m]$ with smooth (low frequency) signal, the high frequencies associated mainly with noise may be removed by a digital filter of the form

$$y_i = c_o x_i + \sum_{j=1}^{n} c_j (x_{i+j} + x_{i-j}), \quad i = n+1 \text{ to } m-n, \qquad (1)$$

where y_i is the filtered value of x_i, and $c = [c_j, j = 1 \text{ to } n]$ are the filter coefficients. A lucid introduction to digital filters is given by Hamming (9). Filters of the form (1) are referred to as nonrecursive (y does not appear on the right side of the = sign), symmetric (x_{i+j} and x_{i-j} are equally weighted), and smoothing (x_{i+j} and x_{i-j} enter as a sum rather than a difference). Notice that n points at either end of $\mathbf{x}$ are not processed in (1), although for comparative graphing and other bookkeeping convenience, some users retain the ends points by the assignment $y_i = x_i$.

Digital filters are commonly characterized by their response functions

$H(f)$. The frequency f is relative to the sampling rate of **x**, which is assumed to be constant. For example, if **x** has a component that repeats every four samples, the frequency of that component is 1/4 in normalized terms. The maximum observable (Nyquist) frequency is 1/2. $H(f)$ is the ratio of the amplitude of f in **y** to its amplitude in **x**. The set of f for which $H(f)$ is near unity (to within some tolerance) is called the pass band, and the set of f for which $H(f)$ is near zero is called the stop band. Regions where $H(f)$ is neither stop nor pass, but is changing from one to the other, are called transition regions.

Filters that stop high frequencies $f \geq f_{stop}$ and pass low frequencies $f \leq f_{pass}$, with one transition region $f_{pass} < f < f_{stop}$, are called low-pass filters. One way to generate a filter with the desired f_{pass} and f_{stop} is to use a filter-design computer program that will generate the coefficients c_j to specification. Another way is to have a set of standard filters that can be used in succession to suppress selected ranges of high frequency. We choose the second way, and in doing so, we reexpress Eq. 1 as

$$\text{If } n(2k-1)+1 \leq i \leq m-n(2k-1)$$

$$\text{then } y_i = c_o x_i + \sum_{j=1}^{n} c_j (x_{i+jk} + x_{i-jk}).$$

$$\text{Otherwise, } y_i = x_i \text{ (i.e. retain unfiltered } x_i), \qquad (2)$$

where k is a positive integer defined below.

If $f_{stop} \leq 1/3$ when $k = 1$, then the following algorithm can stop as broad a range of high frequencies as one pleases:

1. Input data vector **x** and integer *npass*;
2. $k \leftarrow 1$; *jpass* $\leftarrow 1$;
3. **y** $\leftarrow$ filtered **x** by formula (2);

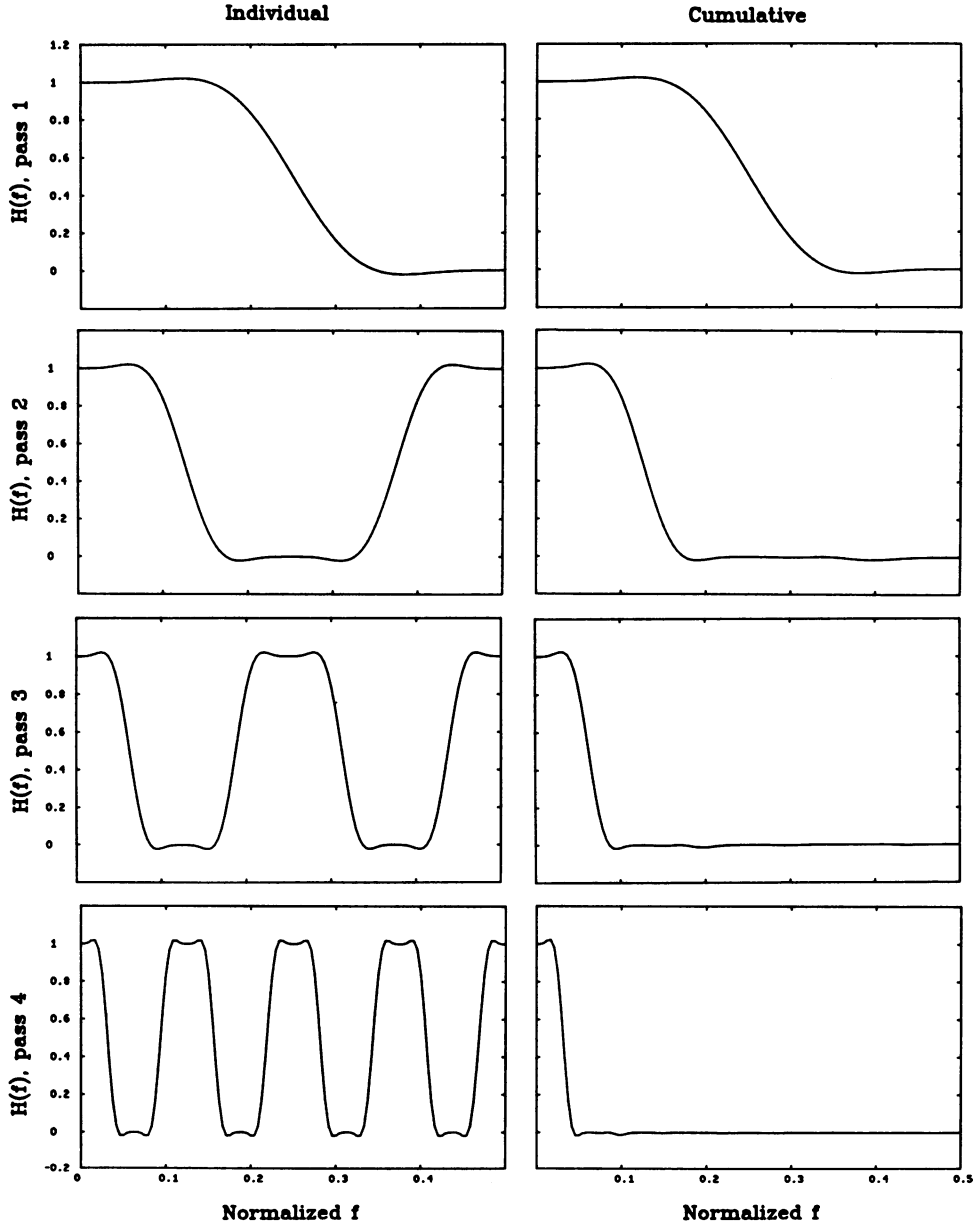

FIGURE 12 Frequency response functions from four passes of the filter in Table III corresponding to $n = 5$. The left column illustrates the response for an individual pass if no other passes are made, as given by Eq. 4. The right column is the cumulative (product) effect of the current and previous passes.

4. $\mathbf{x} \leftarrow \mathbf{y}$; $k \leftarrow 2k$; $j\text{pass} \leftarrow j\text{pass} + 1$;
5. If $j\text{pass} > n\text{pass}$ then stop else go to 3. (3)

Steps 3, 4, and 5 are an iterative loop that is executed $n$pass times. An example is given at the bottom of Table III. The first pass uses the coefficients c_j as in Eq. (A2), with $k = 1$ and $H(f)$ given by

$$H(f) = c_o + 2 \Sigma c_j \cos(jkw), \quad \text{where } w = 2\pi f. \tag{4}$$

A typical plot of H vs. f is shown at the top of Fig. 12. As k is doubled repeatedly in (Eq. A3, step 4), $H(f)$ for each individual pass begins to exhibit periodic behavior as shown in Fig. 1, left column. Note that only the first pass is a low-pass filter. Subsequent passes admit higher frequencies. However, the total effect is determined by the product of the H's of the individual passes as shown in Fig. 1, right column. High frequencies admitted by the second pass have already been stopped by the first pass, and so on. The final result is that each pass divides f_{pass} and f_{stop} by 2. Thus, a very powerful low-pass filter can be produced from a not-so-powerful but very short filter. In addition, this type of filtration by stages is ideal for data exploration. One can filter until all desired high frequency noise is gone or until undesirable signal distortion is detected in the residuals. In the latter case, the stage before distortion occurred is chosen. Two cautions: (Eq. A3, step 3) must be completed before any y_i is put back in x_i, and intermediate loops may not be skipped.

The effect of doubling k in (Eq. A3, step 4) is to double the width of the filter. Where the first pass involves n points on either side, the second involves $2n$ points on either side of x_i, the third involves $4n$ points, and so on. With each pass an increasing number of points will be unfiltered or incompletely filtered at each end of $\mathbf{x}$. After the final pass $n(2^{npass} - 1)$ points at each end are not filtered to specification.

As examples, we choose a family of filters with the general shape of $H(f)$ illustrated at the top of Fig. 1. The relations $H(0) = 1$ and $H(1/2) = 0$ hold exactly with high degrees of tangency at those points. The relation $H(1/4) = 1/2$ also holds, and H has odd symmetry about that point, yielding the advantage that $c_j = 0$ for all even $j > 0$, saving computation. The particular coefficients for four short filters are given in Table III. The ideal value of cumulative H in the pass band is 1, and the ideal value in the stop band is zero. But the form of H in Eq. A4 admits some error, which is specified in the last column of Table III. This error is a maximum deviation from ideal in either the pass or stop band for any number of passes.

One application of filtering is numerical differentiation of the data. Divided difference formulas for the first and second derivatives e.g.,

$$dx_i/dt \sim (x_{i+j} - x_{i-j})/(2j\Delta t) \tag{5}$$

$$d^2x_i/dt^2 \sim (x_{i+j} + x_{i-j} - 2x_i)/(j\Delta t)^2 \tag{6}$$

are notorious amplifiers of high frequency noise. However, when high frequencies are practically absent (e.g., because they were filtered out), the behavior of Eqs. A5 and A6 can be quite tame.

Finally we illustrate that a band-pass filter (one which stops both high and low frequencies outside some intermediate range) can be generated also. The following table of f_{pass} and f_{stop} holds for any filter in Table II.

TABLE II
PASS AND STOP BANDS FOR THE FIRST FOUR FILTERS

	fpass	fstop
pass 1	1/6	1/3
pass 2	1/12	1/6
pass 3	1/24	1/12
pass 4	1/48	1/24

TABLE III
COEFFICIENTS OF SMOOTHING FILTERS*

n	Denominators	Numerators					$H(f)$ Maximum error
		1	3	5	7	9	
3	288	89	−17				0.073
5	288	89	−21	4			0.032
7	1536	475	−120	34	−5		0.016
9	331776	102823	−27041	9109	−2204	257	0.008

For example, for $n = 3$: pass 1, $y_i = x_i/2 + [89(x_{i-1} + x_{i+1}) - 17(x_{i-3} + x_{i+3})]/288$; pass 2, $y_i = x_i/2 + [89(x_{i-2} + x_{i+2}) - 17(x_{i-6} + x_{i+6})]/288$; pass 3, $y_i = x_i/2 + [89(x_{i-4} + x_{i+4}) - 17(x_{i-12} + x_{i+12})]/288$.

*$c_0 = 1/2$, $c_2 = c_4 = c_6 = \ldots = 0$ for all filters.

For example, if we save y for pass 2 as an intermediate result, and subtract y from pass 4, i.e.,

$$\mathbf{y} \leftarrow (\mathbf{y}_{pass2} - \mathbf{y}_{pass4}), \tag{7}$$

the result is to stop $f \leq 1/48$ and $f \geq 1/6$, while passing $1/24 < f < 1/12$. The principle is simple; when two filtered versions of $\mathbf{x}$ are subtracted, the common passed frequencies cancel out (nearly), provided those frequencies are in phase. Since Eq. A1 does not introduce phase shifts, the subtraction is appropriate.

The authors would like to thank David Bickar for calling their attention to the possible involvement of unstirred layers in the "burst" phenomenon studied here, and to Dr. John E. Fletcher of the Laboratory of Applied Studies, Division of Computer Research and Technology for advice concerning the question of diffusion of O_2 through an unstirred layer.

Received for publication 11 April 1986.

REFERENCES

1. Hendler, R. W., O. H. Setty, R. I. Shrager, B. Bunow, J. Fletcher, B. Reynafarje, and A. L. Lehninger. 1985. Real-time measurements and the H^+/O ratio for succinate oxidation. An early H^+ burst. *Fed. Proc.* 44:1081.
2. Hendler, R. W., O. H. Setty, R. I. Shrager, D. C. Songco, and W. S. Friauf. 1983. Instrumentation and procedures for real time measurements of proton motive force, membrane potential, ΔpH, proton extrusion, and oxygen uptake in respiring cells and vesicles. *Rev. Sci. Instrum.* 54:1749–1755.
3. Reynafarje, B., A. Alexandre, P. Davies, and A. L. Lehninger. 1982. Proton translocation stoichiometry of cytochrome oxidase: use of a fast-responding oxygen electrode. *Proc. Natl. Acad. Sci. USA.* 70:7218–7222.
4. Costa, L. E., B. Reynafarje, and A. L. Lehninger. 1984. Stoichiometry of mitochondrial H^+ translocation coupled to succinate oxidation at level flow. *J. Biol. Chem.* 259:4802–4811.
5. Pedersen, P. L., J. W. Greenawalt, B. Reynafarje, J. Hullihen, G. L. Decker, J. W. Soper, and E. Bustamente. 1978. Preparation and characterization of mitochondria and submitochondrial particles of rat liver and liver-derived tissues. *In* Methods in Cell Biology. G. L. Decker, editor. Academic Press, Inc., NY. 411–479.
6. Gornall, A. G., C. J. Bardawill, and M. M. David. 1949. Determination of serum proteins by means of ths buiret reaction. *J. Biol. Chem.* 177:751–766.
7. Crank, J. 1975. The Mathematics of Diffusion. 2nd ed. Oxford University Press. Chapter 8. 137–159.
8. Reynafarje, B. 1985. Biochemical adaptation to chronic hypoxia of high altitudes. *Molec. Physiol.* 8:463–471.
9. Hamming, R. W. 1977. Digital Filters. Prentiss-Hall, Englewood Cliffs, NJ.:W